



CHARACTERISTICS OF THE SECONDARY PARTICLES FROM π^-C INTERACTIONS AT 40 GeV/c IN DIFFERENT NUCLEAR MATTER PHASES

Ts. Baatar, R. Togoo, G. Sharkhuu, B. Otgongerel

Institute of Physics and Technology, Mongolian Academy of Sciences

E-mail: baatar1945@yahoo.com

ABSTRACT

In this paper we have presented the angular and momentum characteristics of the secondary particles from π^-C -interactions at 40 GeV/c in different phase transition regions of nuclear matter.

INTRODUCTION

The investigation of the multiparticle production in hadron-nucleus, nucleus-nucleus interactions at high energies and large momentum transfers is very important for understanding the strong interaction mechanism and inner quark-gluon structure of nuclear matter.

During the last years the possibility of the observing of the collective phenomena such as the cumulative particle production [1], the production of nuclear matter with high densities, the phase transition from the hadronic matter to the quark-gluon plasma state is widely discussed in the literature [2-5, 11-14].

According to the different ideas and models, if exist these phenomena in the nature, then they will be observed in the hadron-nucleus and nucleus-nucleus interactions at high energies and large momentum transfers and should be influenced to the dynamics of interaction process and would be reflected in the angular and momentum characteristics of the reaction products.

To study the phase transition of nuclear matter we must choose the variables corresponding to this physical process. In the

theoretical calculations are mainly used the effective temperature T , the density of nuclear matter ρ / ρ_0 or the quark chemical potential μ . But the variables ρ and μ are not fully determined experimentally and their values are usually remained model dependently.

In our previous paper [13] we are proposed to study the phase transition process of nuclear matter to use the variable called “the cumulative number”, n_c instead of the variable ρ (or μ).

The cumulative number, n_c in the fixed target experiments is determined by the next formula:

$$n_c = \frac{P_a * P_C}{P_a * P_b} \cong \frac{E_c - P_{ll}^c}{m_p}$$

Here P_a , P_b and P_c are the four dimensional momenta of the incident particle, target and the considering secondary particles correspondingly. E_c is the energy and P_{ll}^c is the longitudinal momentum of the considering secondary particle, m_p is the proton mass. From this formula we see that this variable is a relativistic invariant and can be fully determined experimentally without model dependent. This variable (n_c) may be

interpreted as minimal target mass, which is required for producing of the given secondary particle. We would like to stress that the connection of the variable and the four momentum transfer t is determined by the next formula [13].

$$t = -Q^2 = -(P_a - P_b)^2 = -m_a^2 - m_b^2 + 2E_a \cdot \frac{m_p}{m_p} \cdot (E_c - P_{II}^c) \cong S_{\pi^-p} \cdot n_c \quad (2)$$

Where S_{π^-p} is the total energy square of $\pi^- + p$ - interaction and is determined by the next formula:

$$S_{\pi^-p} = (P_{\pi^-} + P_p)^2 = m_{\pi^-}^2 + m_p^2 + 2E_{\pi^-} \cdot m_p \cong 2E_{\pi^-} \cdot m_p \quad (3)$$

In the fixed target experiment S_{π^-p} is a constant and in our case

$$S_{\pi^-p} \cong 2 \cdot E_{\pi^-} - m_p \cong 75 \text{ GeV}^2$$

The transverse energy spectra of the secondary particles in the different intervals are approximated by exponential functions of the next form:

$$\frac{1}{2 \cdot E_t} \frac{\Delta N}{\Delta E_t} \sim e^{-b \cdot E_t}, \quad E_t = \sqrt{p_t^2 + m^2} \quad (4)$$

The effective temperature T is determined as the inverse of the slope parameters b ,

$$T = \frac{1}{b} \quad (5)$$

EXPERIMENTAL METHOD

The experimental material was obtained with the help of Dubna 2-meter propane (C_3H_8) bubble chamber exposed by π^- - mesons with momentum $40 \text{ GeV}/c$ from Serpukhov accelerator. According to the advantage of the bubble chamber experiment, all distributions in this paper are obtained in the condition of 4π geometry of secondary particles.

The average error of the momentum measurements is $\sim 12\%$ and the average error of the angular measurements is $\sim 0.6^\circ$.

All secondary negative particles are

taken as π^- - mesons. The average boundary momentum from which π^- -mesons were well identified in the propane bubble chamber is $\sim 70 \text{ MeV}/c$. In connection with the identification problem between energetic protons and π^+ -mesons, protons with momentum more than $\sim 1 \text{ GeV}/c$ are included to the π^+ -mesons.

The other experimental details are described in [8,9].

8791 π^-C interactions are used in this analysis.

PHASE DIAGRAMS FOR π^- -MESONS AND PROTONS

In our paper [13] we are presented the dependences between temperature T and cumulative number for negative pions (Fig.1) and protons (Fig.2) from π^-C - interactions at $40 \text{ GeV}/c$. Our analysis showed that dependence

of the temperature T on the variable n_c (or t), the strongly interacting matter may occur in three different phases for π^- mesons: hadronic, thermodynamic equilibrium and quark-gluon plasma (QGP) and in two different phases for

protons: thermodynamical equilibrium and QGP states.

The main goal of this paper is to present the angular and momentum characteristics of negative pions and protons from π^-C interactions in these different phases.

In the case of protons as mentioned above we are worked in the momentum interval from

$\sim 0,150 \text{ GeV}/c$ to $\sim 1,0 \text{ GeV}/c$ and the protons with momentum $P_p > 1 \text{ GeV}/c$ which gives the main contribution to the hadronic phase are included inside π^+ mesons as mixture. This methodical difficulty may be the main reason of why we don't see the hadronic phase for the secondary protons.

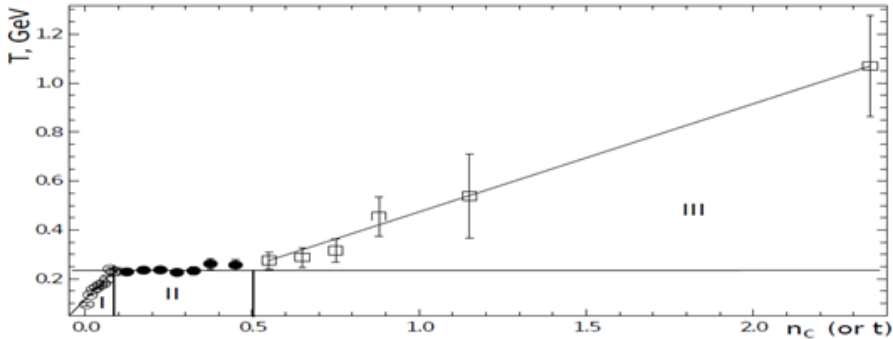


Figure 1: Shows the phase diagram of π^- -mesons produced from π^-C -interaction at $40\text{GeV}/c$.

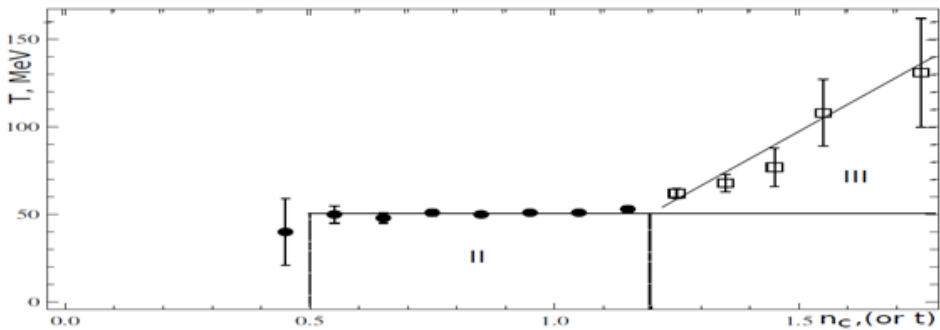


Figure 2: Shows the phase diagram of protons produced from π^-C -interaction at $40\text{GeV}/c$.

$\pi^- + C \rightarrow \pi^- + X$ ANALYSIS

To do the comparative analysis, the angular and momentum characteristics of the all secondary π^- - mesons from π^-C -

interactions at $40 \text{ GeV}/c$ are presented on Fig.3. The average values of these distributions are given in table 1.

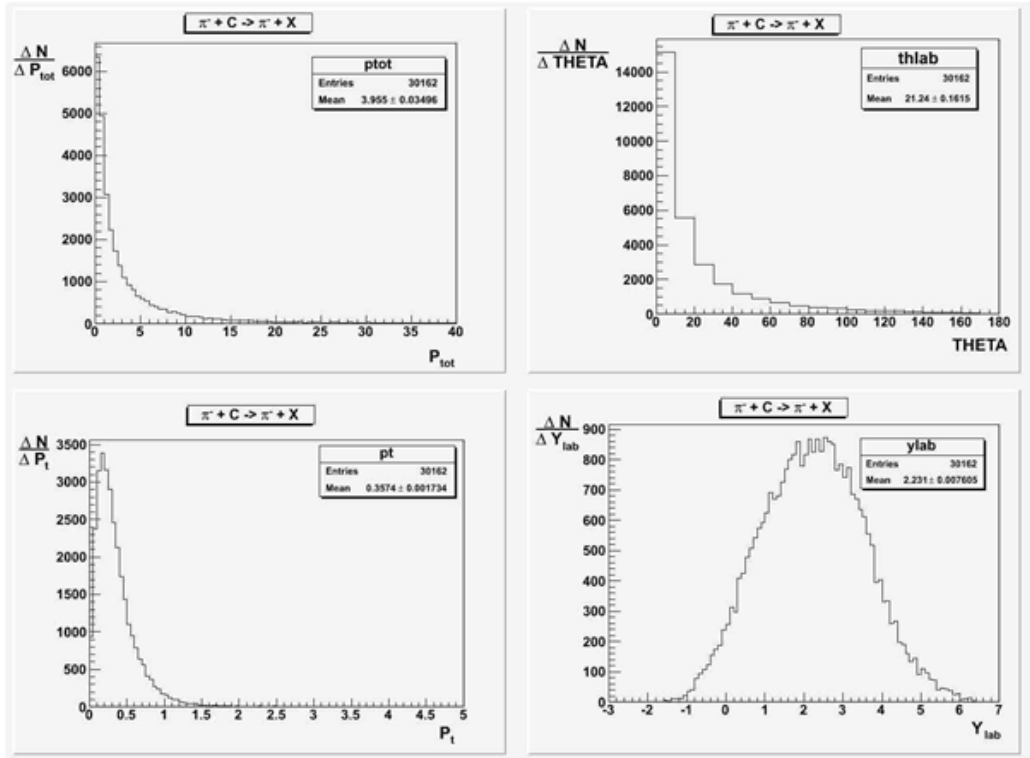


Fig.3 shows the momentum (P_{tot}), angular (Θ), transverse momentum (P_t) and rapidity (Y_{lab}) distributions for all π^- -mesons from $\pi^- C$ interactions at 40 GeV/c.

Table 1 (for π^- mesons)

| Average characteristics | Number of π^- mesons | $\langle P_{tot} \rangle$ (GeV/c) | $\langle \Theta_{lab} \rangle$ (in degrees) | $\langle P_t \rangle$ (GeV/c) | $\langle Y_{lab} \rangle$ |
|--|--------------------------|-----------------------------------|---|-------------------------------|---------------------------|
| All π^- mesons | 30162 | $3,955 \pm 0.035$ | $21,24 \pm 0,16$ | $0,357 \pm 0,002$ | $2,231 \pm 0,008$ |
| π^- mesons with $n_c \leq 0.08$ and $T < 0.200$ Gev | 19702 | $5,431 \pm 0,039$ | $7,00 \pm 0,05$ | $0,313 \pm 0,002$ | $2,924 \pm 0.020$ |
| π^- mesons with $0.08 \leq n_c \leq 0.5$ and $T \approx 0,220$ Gev | 9879 | $1,174 \pm 0,012$ | $45,15 \pm 0,45$ | $0,419 \pm 0,004$ | $0,987 \pm 0,010$ |
| π^- mesons with $n_c > 0.5$ and $T \geq 0,220$ Gev | 581 | $1,547 \pm 0,064$ | $97,44 \pm 4,00$ | $0,930 \pm 0,038$ | $-0,115 \pm 0,005$ |

Fig.4 shows the angular and momentum distributions (total momentum P_p , angle transverse momentum and rapidity Y_{lab}) of

π^- mesons which correspond to the hadronic phase (the I region with $n_c \leq 0,07$, $T < 0,200$).

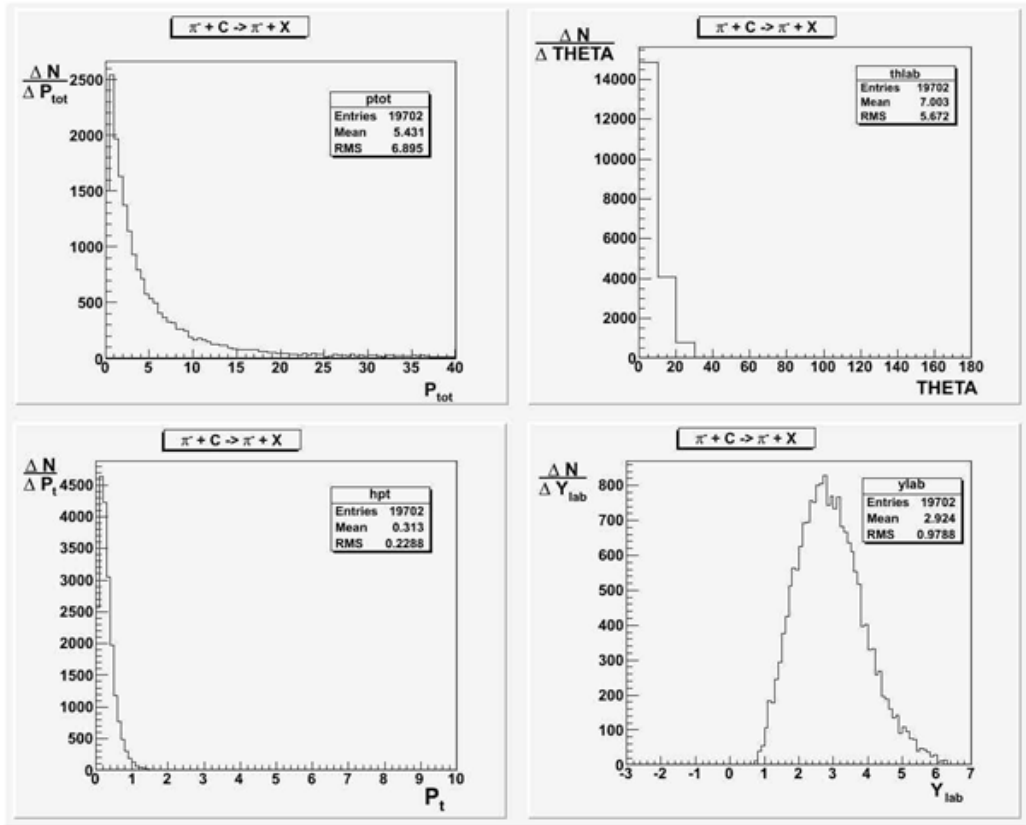


Fig.4 shows the angular and momentum characteristics of π^- -mesons in the hadronic phase (I region).

Angular and momentum distributions of π^- mesons which correspond to the phase transition region from the hadronic matter to the QGP phase for which the temperature T

remains practically constant (the II region with $0,07 > n_c \leq 0,5$, $T \approx 0,220 \text{ GeV}$) are shown on Fig.5.

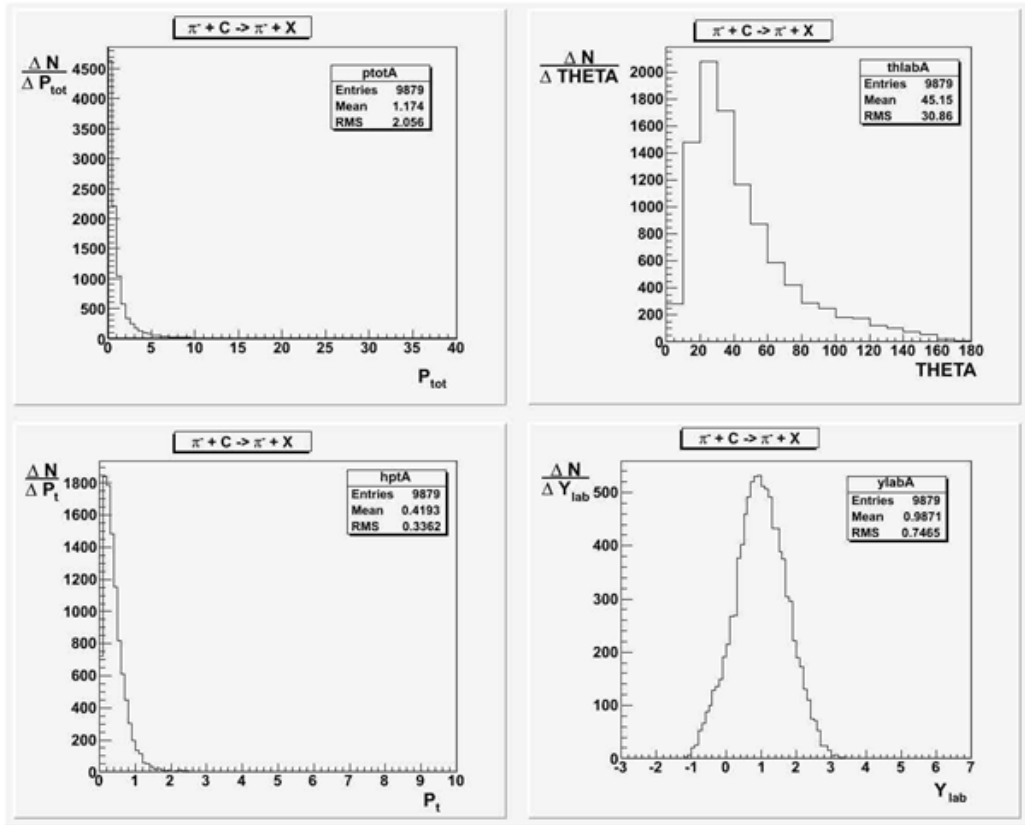


Fig.5 shows the angular and momentum characteristics of π^- -mesons in the mixed phase (II region).

Fig.6 shows the same distributions of π^- -mesons which belong to the QGP state (the III region with $n \geq 0,5$, $T \geq 0,220$ GeV). For π^- -mesons produced in this region we are obtained $\langle Y_{lab} \rangle = -0,115 \pm 0,005$ and $\langle P_t \rangle =$

$0,930 \pm 0,038$ GeV/c. So we would like to stress that π^- -mesons only produced in the target fragmentation region with comparatively large transverse momentum are included in this region.

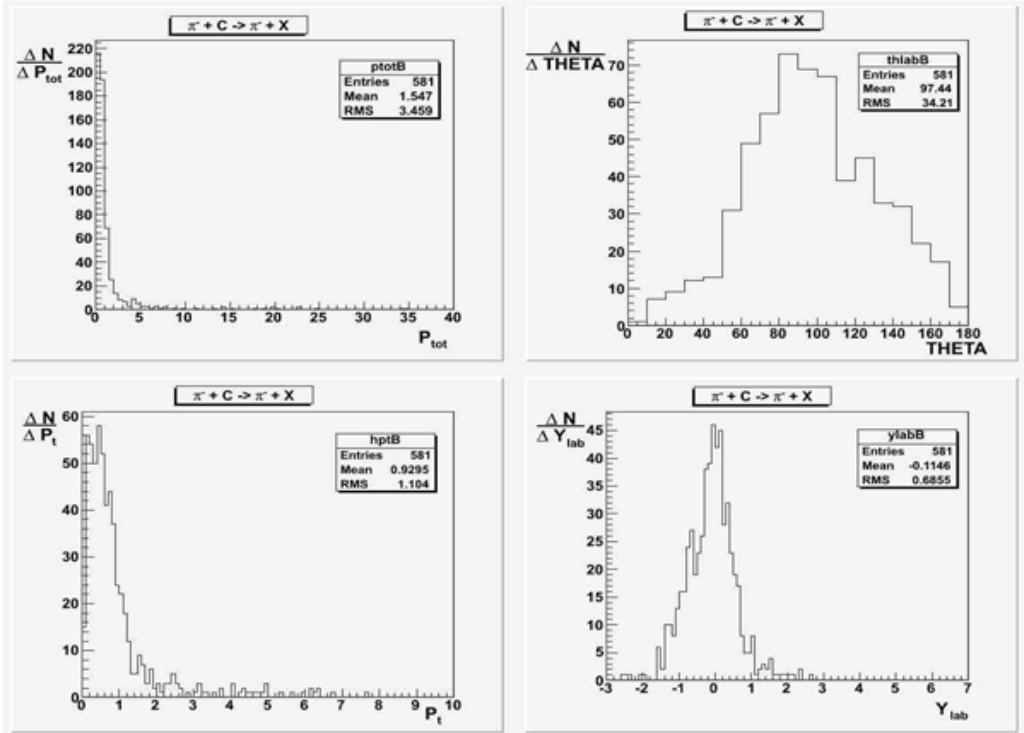


Fig.6 shows the angular and momentum characteristics of π^- -mesons in the QGP phase (III region).

First of all we would like to stress that the exact separation of the transition regions from the hadronic matter to the mixed phase

and from the mixed phase to the QGP should be considered carefully. This separation procedure needs more detailed studies.

$\pi^- + C \rightarrow P + X$ ANALYSIS

With the goal of comparison, the angular and momentum characteristics of all secondary

protons from $\pi^- C$ - interactions at 40 GeV/c are presented on Fig.7.

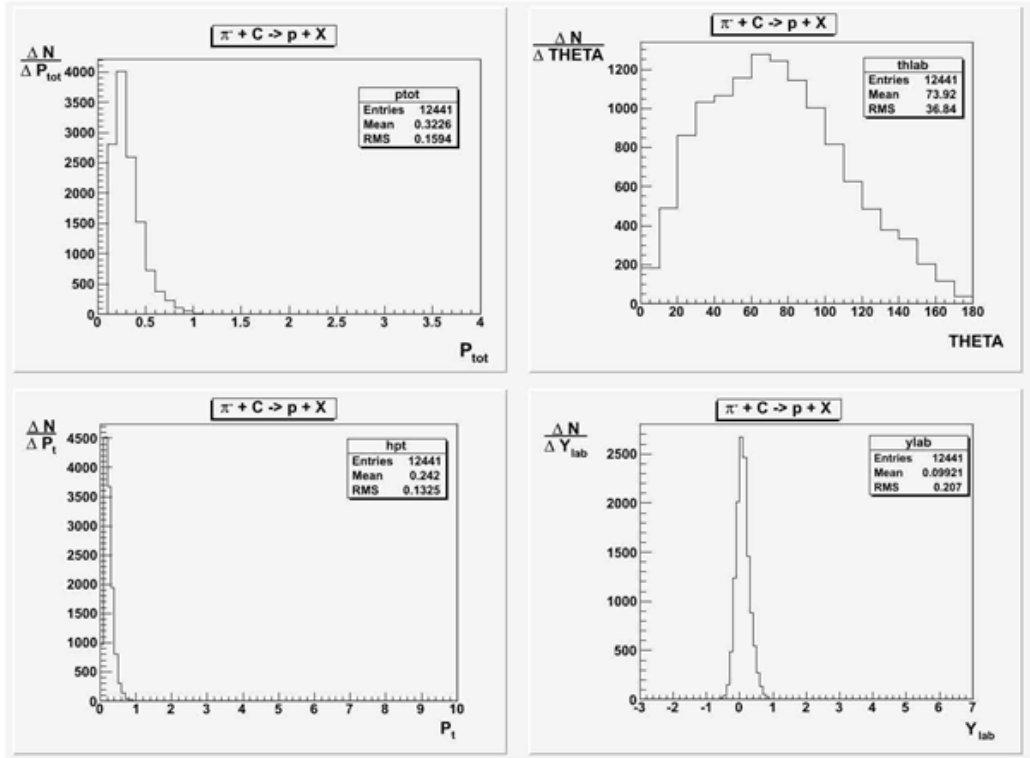


Fig.7 presents the momentum (P_{tot}), angular (Θ), transverse momentum (P_t) and rapidity (Y_{lab}) distributions of all protons from $\pi^- C$ interactions at 40 GeV/c.

Fig.8 shows the corresponding angular and momentum characteristics of protons in the mixed phase (the II region).

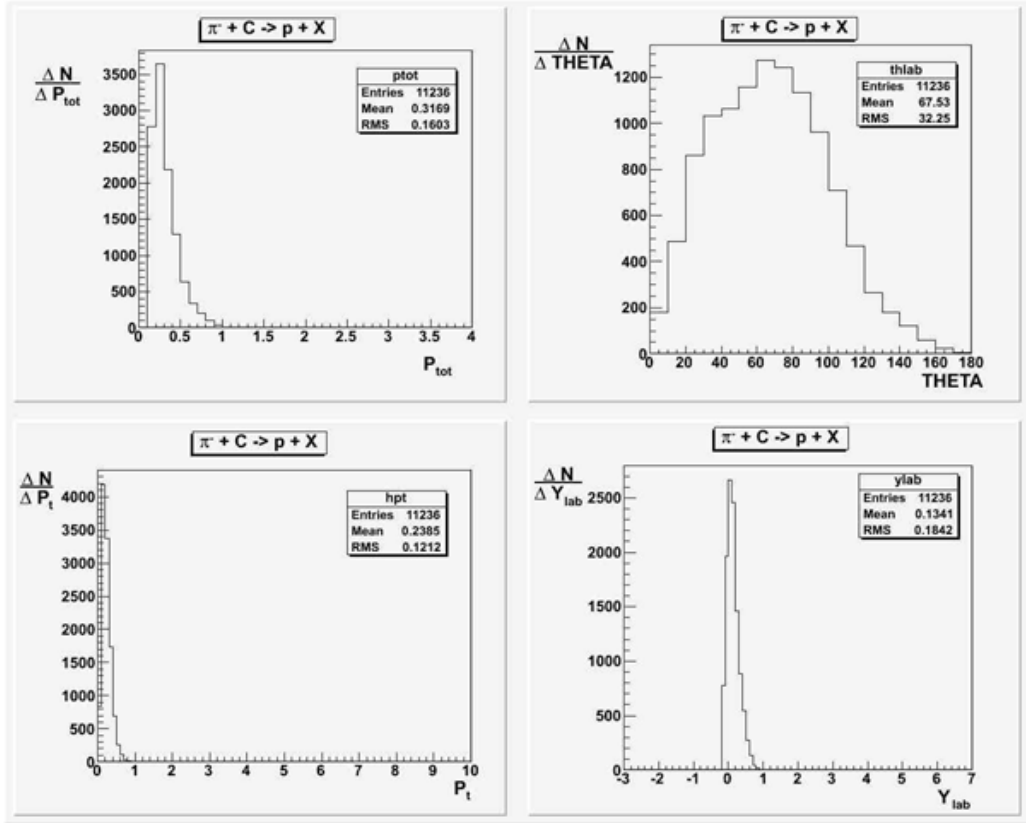


Fig.8 shows the angular and momentum characteristics of protons in the mixed phase (II region).

Table 2 shows average values of angular and momentum characteristics of all protons and protons in the two other different regions.

Table 2 (for protons)

| Average characteristics | Number of protons | $\langle P_{tot} \rangle$ (Gev/c) | $\langle TH_{lab} \rangle$ (in degrees) | $\langle P_t \rangle$ (Gev/c) | $\langle Y_{lab} \rangle$ |
|---|-------------------|-----------------------------------|---|-------------------------------|---------------------------|
| all protons | 12441 | $0,323 \pm 0,003$ | $73,92 \pm 0,66$ | $0,242 \pm 0,002$ | $0,099 \pm 0,001$ |
| protons with $n_c \leq 1.2$ and $T \approx 0.050$ Gev | 11236 | $0,317 \pm 0,003$ | $67,53 \pm 0,64$ | $0,238 \pm 0,002$ | $0,134 \pm 0,001$ |
| protons with $n_c > 1.2$ and $T \geq 0.050$ Gev | 1205 | $0,376 \pm 0,011$ | $133,4 \pm 3,84$ | $0,275 \pm 0,008$ | $-0,223 \pm 0,006$ |

Fig. 7, 8 and Table 2 show that average values of the angular and momentum characteristics of protons in the mixed phase show small differences in comparison with data for all protons. Of course this is connected with the fact that about 90 % of protons produced in the mixed phase.

Fig. 9 and Table 2 show that $\langle P_{tot} \rangle$, $\langle P_t \rangle$ and $\langle TH_{lab} \rangle$ in the III region are increased and $\langle Y_{lab} \rangle$ is decreased in comparison with the data for all protons and protons in the III region, in other words, protons which produced at large momentum transfers, t , are included in this region.

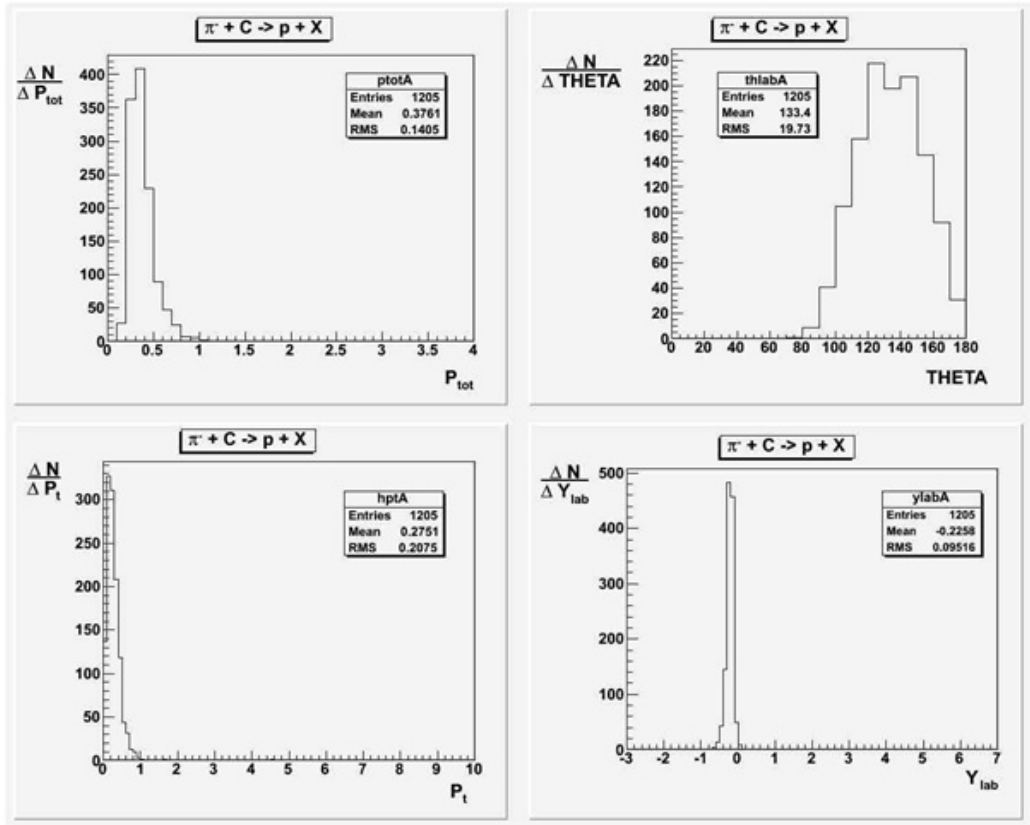


Fig.9 shows the angular and momentum characteristics of protons in the QGP phase (III region)

CONCLUSION

Our analysis showed that angular and momentum characteristics of π^- mesons and protons from π^-C interactions at 40 are different in every region.

We note that π^- mesons which produced in the projectile fragmentation region give the main contribution to the hadronic phase

and π^- mesons produced only in the target fragmentation region with large transverse momentum are included to quark-gluon plasma (QGP) phase. All other π^- mesons with average characteristics between I and III regions are included to the mixed phase with the constant temperature $T=T_c$.



REFERENCES

- [1] Baldin A.M., Particles and Nuclei., 1977, 8, p.429.
- [2] J.C. Collins and M.J. Perry., Phys. ReV. Lett., 34(1975), 1353.
- [3] Polyakov A.M., Phys. Lett. B59, 1975, 82.
- [4] Polyakov A.M., Phys. Lett. B72, 1978, 477.
- [5] Gavani R.V. and Sats H., Phys. Lett. B145, 1984, 248.
- [6] Baatar Ts. et al., JINR, p1-89424, Dubna, 1989.
- [7] Baatar Ts. et al., Journal of Nuclear Physics, 52, 3(9), 1990.
- [8] Balea O. et al., Phys. Lett. B39, 571, 1972.
- [9] Abdurahmanov A.J. et al., JINR, p1-6937, Dubna, 1973.
- [10] N. Angelov et al., JINR p1-9209, Dubna, 1975.
- [11] R.Hagedorn Nouvo Cim. Suppl. 3, 147 (1965).
- [12] Dirk H. Rischke. arXiv:nucl-th/0305030v2.
- [13] Baatar.Ts et al., JINR, E1-2012-13, Dubna, 2012.
- [14] Ramona Vogt, "Ultrarelativistic Heavy-Ion Collisions", Berkeley, CA, USA, 2007.
- [15] Baatar.Ts et all, Proceedings of the XXI International Conference on QCD and Relativistic Nuclear Physics, 2012, Dubna.